EUROREGIO BNAM2022
Joint Acoustics Conference
9th-11th of May, Aalborg, Denmark

Measured and Computed Reflection from a Finite Plate

Sondre Utmo Vikøren[1,*], **U. Peter Svensson**[1]

[1]Acoustics group, Dept. of Electronic Systems, Norwegian University of Science and Technology, Trondheim, Norway.

[*]sondre.u.vikoren@ntnu.no

Abstract

Inaccuracies in computation of sound propagation through complex geometries are related in part to inadequate modelling of edge diffraction. Prediction methods need to be evaluated against reference results which could be benchmark measurements, of adequate accuracy. This paper presents impulse response measurements for a rigid 1x1m plate in an anechoic room. The plate was made of 20 mm plywood with a smooth and hard surface. The measurements used a 25 mm diameter tweeter as a source and a 1/2-inch microphone. Using fixed source and receiver positions, the plate was suspended from the ceiling, and rotated in steps of 15 degrees around its vertical symmetry axis. This gave cases with and without specular reflections, with and without direct sound. A signal-to-noise ratio larger than 30 dB was found for the frequency range of 125 Hz to 20 kHz. Calculations were made with the Matlab Edge diffraction toolbox, modeling the loudspeaker as a point source, and the plate as thin or thick. Measured and predicted 1/6-th octave band levels were compared and for the 1/6-th octave band from 125 Hz to 16 kHz, and across 12 plate rotation angles, the 2.5% and 97.5% percentiles and median values were computed. For one of the two setups, using a thick plate model and diffraction order 3, the percentile values were -1.1 dB and +1.8 dB, respectively, with a median value of 0.36 dB. For diffraction order 2, and a thick plate model, these results were only marginally worse, with the percentile values -1.4 dB and +1.8 dB.

Keywords: Edge-diffraction, measurements, simulations

1 Introduction

Geometrical acoustics (GA) is the dominating computational method in room acoustics, and outdoors in city environments [1]. A major challenge is that GA can not handle finite reflectors, but edge diffraction modeling can improve that [2]. Other, more accurate, methods such as BEM, FEM, FDTD, are too computationally demanding for many cases, with computational load scaling poorly with problem size and frequency.

The addition of edge diffraction modeling adds significantly to the complexity of GA software. How important is it? Some benchmarks were published recently [3] that included some cases that were particularly testing different software algorithms' abilities to handle edge diffraction. Measurements and simulations with different GA softwares were presented. The differences between measurements and simulations were quite substantial already for such a simple case as reflection from a finite rigid plate. A finite rigid plate is a classical test case which has been studied earlier [4], and simplified modeling approaches have been suggested as well [5].

The goal of this paper is to compare carefully conducted measurements of scattering from a rigid plate, with calculations made with the freely available edge diffraction Matlab toolbox [6].

2 Theory

As an extension of GA the Edge Source Integral Equation (ESIE) method decomposes a soundfield generated by a convex scattering object into three components, namely the direct (p_{dir}), the specular reflected (p_{spec}) and

the diffracted sound pressure components of first and higher orders (p_{FOD}, p_{HOD})[7].

$$p = p_{\mathrm{dir}} + p_{\mathrm{spec}} + p_{\mathrm{FOD}} + p_{\mathrm{HOD}} \tag{1}$$

The direct sound and specular reflections are the same components as calculated by GA methods. The first-order diffraction term, p_{FOD}, is computed for all edges that are visible from both the source and the receiver, using time-domain [8] or frequency-domain expressions [9]. The final term, p_{HOD}, can be computed in two ways. A time-domain order-by-order method can be used for low orders of diffraction [2], while an integral equation formulation can be used to compute arbitrarily high diffraction orders for convex objects using a frequency-domain formulation [7]. The order-by-order method has a computational cost which increases exponentially with diffraction order whereas the integral equation formulation has a computational cost which grows linearly with diffraction order, with a higher ”startup cost”.

These calculations are implemented in to various degrees in the edge diffraction Matlab toolbox version B1 [10] as well as in the version 0.216 [6]. In this study, only low orders of diffraction will be used, which means that time-domain calculations, using the order-by-order method, are more efficient than the frequency-domain integral equation method. The time-domain first-order diffraction is computed with a numerical integration scheme which is very accurate for low frequencies and with a gradually reduced accuracy for high frequencies. Therefore, a high sampling frequency is typically used. For the second- and higher-order time-domain diffraction calculations, each edge is pre-divided into elements that are made larger for each higher diffraction order. For second- and higher-order diffraction, each element’s contribution is computed for the center points of the elements. Calculation settings are specified below.

3 Scattering measurements

The measurements were performed in the anechoic chamber at NTNU Gløshaugen. The setup consisted of a 1-inch dome tweeter (SEAS®H614) as sound source, a 1/2-inch microphone (Brüel & Kjær®4190) and a 1x1 m plywood plate with 20 mm thickness. The plywood plate had phenolic resin smooth surface layers, and strips of plexiglass were glued to the cut edges. Figs. 1 a) and b) show the geometry of the setup. The loudspeaker element was screwed to a horizontal metal rod and the microphone was placed at the end of a horizontal metal tube. Between the source and receiver the plate was suspended from the ceiling by two metal wires.

The software AFMG Easera®, version 1.2.16.4, and a Lynx Aurora®audio interface, were used to measure impulse responses, using exponential sine sweeps, ”chirps”, as stimuli. Chirps covered the full range from 0 Hz to half the sampling frequency, which was 44.1 kHz. The recommended frequency range for the used tweeter is 3 kHz to 25 kHz, but here the tweeter was used down to around 118 Hz. A low amplitude was used so that repeated measurements did not show any trend in frequency response amplitude, for the frequency range of interest. A trend of increasing or decreasing magnitude, over time, could have indicated heating effects in the voice coil or suspension.

The measurements were performed for 12 different plate positions. The different positions consisted of rotating the plate around its central vertical axis in 15 degree increments. For each plate position impulse responses were measured with two different combinations of source-receiver positions. Source-receiver position one had both the source and the receiver placed at the same height as the centre of the plate. Source-receiver position two had the source being 125 mm higher than the centre of the plate while the receiver was placed 250 mm lower. Figure 2 illustrates this. Additionally, for both source-receiver positions, the impulse response was measured without the plate. The used loudspeaker is small but with a directivity which increases with frequency. For the setup shown in Figs. 1 a) and b), the largest radiation angle which reaches the plate is around 30 degrees relative to on-axis radiation. The directivity for the same type of loudspeaker was measured in a previous study [11], averaged across octave-band-wide frequency ranges, at a few distinct angles and frequencies, as reproduced in Table 1.

Table 1: Octave-band-wide directivity values for the used loudspeaker element, at the non-standard center frequencies as indicated.

Radiation angle [deg.]	**625 Hz**	**1.25 kHz**	**2.5 kHz**	**5 kHz**	**10 kHz**	**20 kHz**
0°	0 dB	0 dB	0 dB	0 dB	0 dB	0 dB
10°	-0.1 dB	0.0 dB	-0.2 dB	0.0 dB	-0.5 dB	-1.4 dB
20°	-0.4 dB	+0.2 dB	-0.6 dB	-0.6 dB	-1.7 dB	-6.0 dB
30°	-0.6 dB	+0.3 dB	-1.1 dB	-1.6 dB	-3.4 dB	-15.9 dB

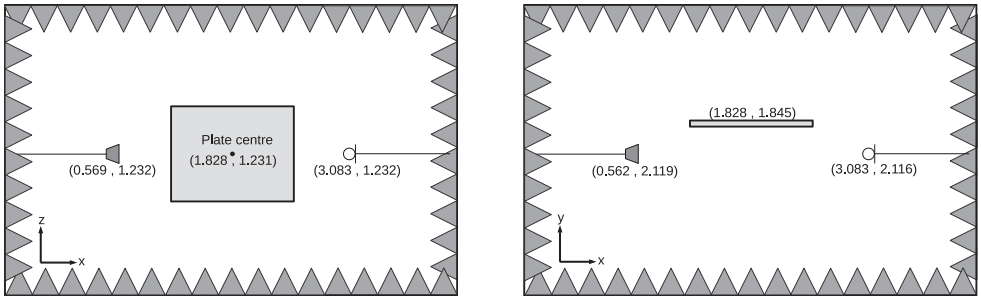

(a) (b)

Figure 1: Coordinates of physical measurement setup. (a) xz-plane. (b) xy-plane

4 Numerical simulations

The numerical simulations were performed with the Edge Diffraction Matlab toolbox version B1, and executed with Matlab 2021a. The most essential settings used for the calculations are summarized in table 2. Here the ”element size” gives the number of elements per wavelength for the shortest wavelength (i.e., at half the sampling frequency). As mentioned in the Theory chapter, first-order diffraction uses another integration scheme than higher-order diffraction.

The toolbox uses omnidirectional sound sources with an ideal Dirac impulse response in the computations. As can be seen in Table 1, the (octave-band wide) directivity of the measurement loudspeaker is within [-0.6,0] dB for a large part of the spectrum and radiation angles. The increasing directivity for high frequencies and large radiation angles will certainly limit the accuracy of the numerical simulations, but to a small degree. To remove the influence of the measurement loudspeaker’s non-flat frequency response, all measured frequency responses (transformed from the measured impulse responses using the discrete Fourier transform) were divided by the free-field loudspeaker response, which largely eliminated the effects of the loudspeaker’s response. The same was done for the simulations, which made the measured and simulated relative responses comparable. However, a time windowing was used before transforming the measured impulse responses to frequency responses (see subsection 1), and this windowing will inevitably affect the response, and primarily the low-frequency end of the response. To get similar effects for the simulated responses, the simulated impulse responses were convolved with *a model* of the measurement loudspeaker. A model was used, rather than the measured response, in order to remove the effects of noise and small scattering details that might change with radiation direction.

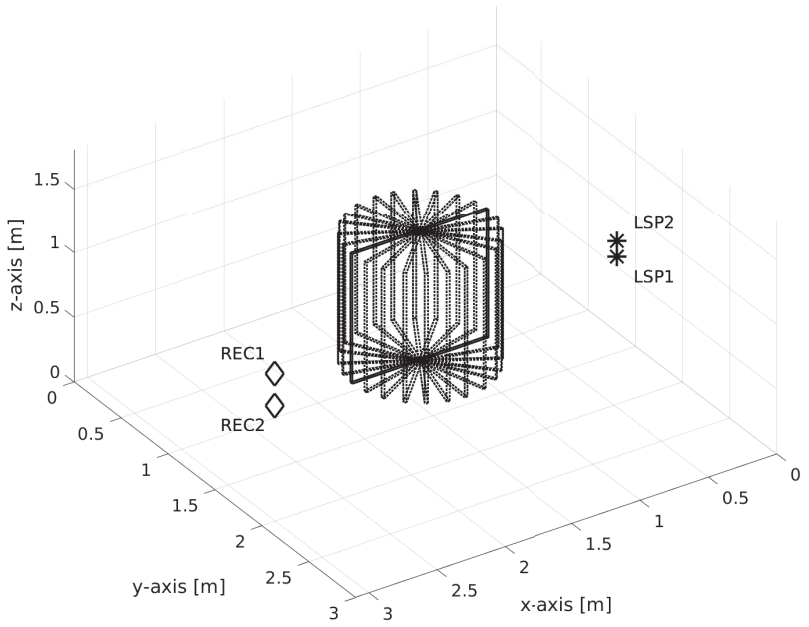

Figure 2: Measurement setup. All plate angles indicated. LSP1 and LSP2 refer to the source position for setup 1 and 2 respectively. Similarly REC1 and REC2 refer to the receiver position for setup 1 and 2. For setup 1, both source and receiver had the same z-coordinate as the plate centre, i.e. no vertical difference between the two positions. For setup 2, the source was shifted 125 mm in positive z-direction while the receiver was shifted 250 mm in negative z-direction direction, making the vertical difference between the two 375 mm.

4.1. Developing a model of the measurement loudspeaker

The free-field impulse response was measured in the main direction. A short window was applied before transforming the impulse response to a frequency response.

An IIR filter was fit to the magnitude of the frequency response, as follows. First, a second-order high-pass filter was designed by tweaking manually the cutoff frequency and the Q-value. Then a third-order IIR filter was fit to the difference between the measured response and the modeled high-pass filter response, using Matlab's `yulewalk` function. Finally, an extra second-order low-pass filter at 22 kHz was introduced. These filters could be combined to an 7-th order IIR filter. The results are shown in Fig. 3. Since the measured response was up-sampled from a sampling frequency of 44.1 kHz to 88.2 kHz (which was the sampling frequency of the simulations), a very steep fall-off can be observed above 22 kHz. In Fig. 3 (a) a small fraction of a sample time difference can be observed between the measured IR and model IR, since no attempt was made to adjust the delay of the model impulse response to less than integer samples.

The window used for this free-field response is also indicated in Fig. 4 (a): a 10-sample long half-Hanning window started at 200 samples (2.27 ms) before the max peak of the measured impulse response. At the end, a 100 samples long (1.1 ms) half-Hanning window ended 3 ms after the max peak.

Table 2: Key settings used in the toolbox

Variable	Value
Sound speed [m/s]	342.74
Sampling rate [Hz]	88200
Diffraction order	1-3
Element size (1./2./3. diffraction order)	-/1/0.5 elements per shortest wavelength

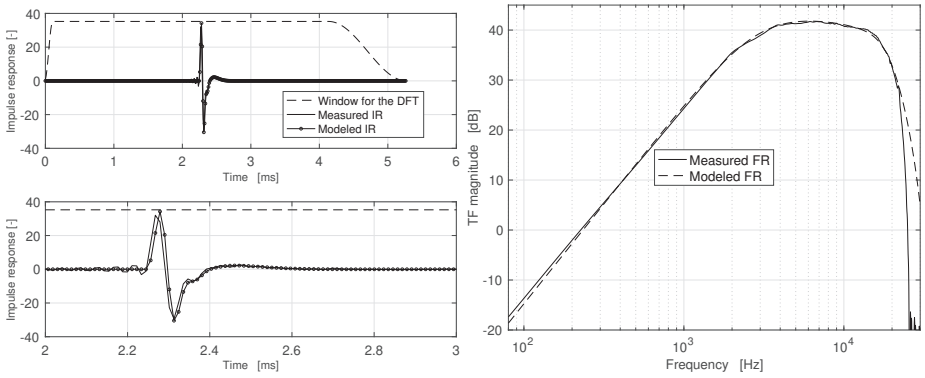

(a) (b)

Figure 3: (a) The measured impulse response of the loudspeaker used in the scattering measurements, and the model impulse response, with the used window indicated, and (b) the corresponding frequency responses.

5 Processing results

5.1. Windowing the measured response

To get as comparable results as possible, both the measured and the simulated IRs were windowed before transforming them to the frequency domain via a discrete Fourier transform (DFT). Prior to the windowing, the simulated IRs were convolved with a loudspeaker model IR described in section 4. The peak of the impulse response was detected and 2.27 ms before, and 12 ms after, the peak were kept. In addition, a half Hanning window of length 0.11 ms (10 samples) was applied at the start, and another half Hanning window of length 1.1 ms (100 samples) was applied to the end of the window, as illustrated in Fig. 4.

Examples of simulated and measured frequency responses are shown in Fig. 5. They were computed using a DFT size which gives a frequency resolution of 1 Hz. The measured noise was determined by repeating an impulse response measurement without sending an excitation signal to the loudspeaker. From this single noise sample, it seems like a signal-to-noise ratio of at least 40 dB results from around 200 Hz, and at least 30 dB from around 100 Hz.

5.2. Fractional-octave band smoothed responses

Rather than analyzing the difference between the simulated and measured narrowband frequency responses in Fig. 5(b), the fractional octave-band smoothed versions are analyzed instead. $H(\omega_k)$ denotes the (complex-valued) frequency response for the set of discrete angular frequencies ω_k, and $H^2(\omega_b)_{1/n}$ denotes the $1/n$-

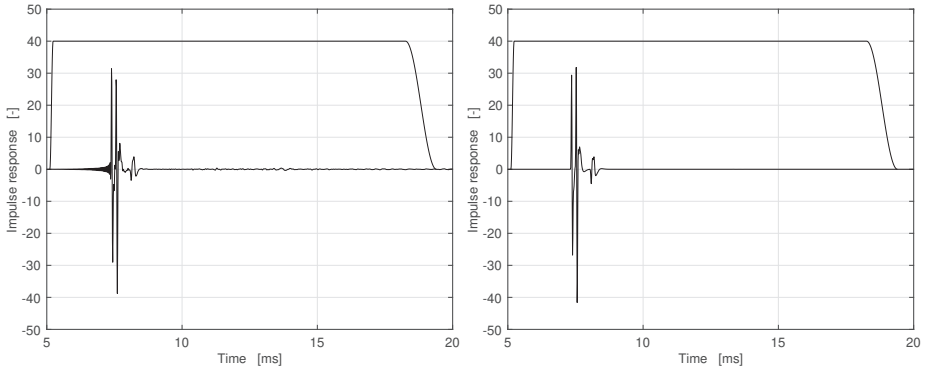

(a) (b)

Figure 4: An example of (a) a measured impulse response and (b) the corresponding simulated impulse response, both with the used window indicated. The simulated impulse response has been convolved with a model impulse response that mimics the loudspeaker response.

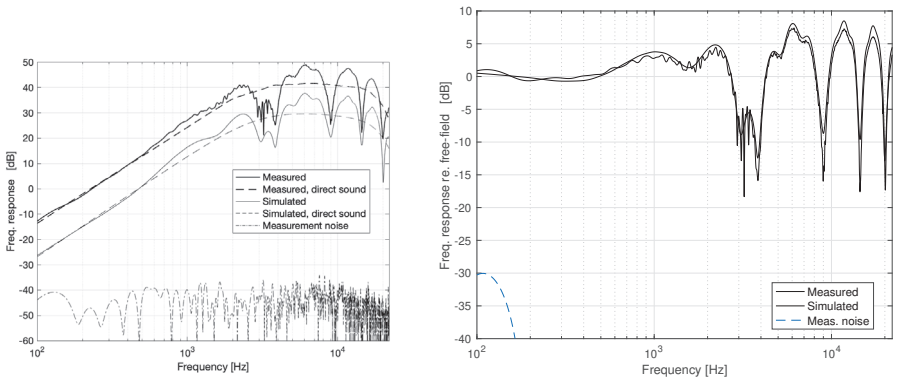

(a) (b)

Figure 5: An example of (a) measured and simulated frequency responses, and (b) frequency responses relative to the direct sound (= free-field response), for the same case as in Fig. 4. The simulated response includes the high-pass filter response that roughly mimics the loudspeaker response. The measured noise is computed from an IR measurement and processing, without sending an excitation signal to the loudspeaker.

octave-band smoothed version, calculated for the $1/n$-octave-band center frequencies ω_b,

$$H^2(\omega_b)_{1/n} = \frac{1}{N}\sum_{k=1}^{N} |H(\omega_k)|^2$$

where the summation is understood to include the frequency bins that fall within each fractional octave band. Thus, the relative smoothed responses are given by

$$H^2(\omega_b)_{rel.,1/n} = \frac{H^2(\omega_b)_{1/n}}{H^2(\omega_b)_{direct,1/n}}.$$

It is very common to use 1/3rd-octave band levels in acoustical measurements. Here 1/6th-octave band smoothing has been used to get more detailed comparisons.

6 Results

To display the difference between the two different measurement setups, Fig. 6 shows the median and the 97,5 and 2,5 percentiles of the differences between measured and simulated fractional-octave band levels for the two different measurement setups. Each dataset, for which the statistical parameters are computed, involves 12 plate angles and 43 1/6-th octave bands (125 Hz - 16 kHz), that is, 516 individual level differences.

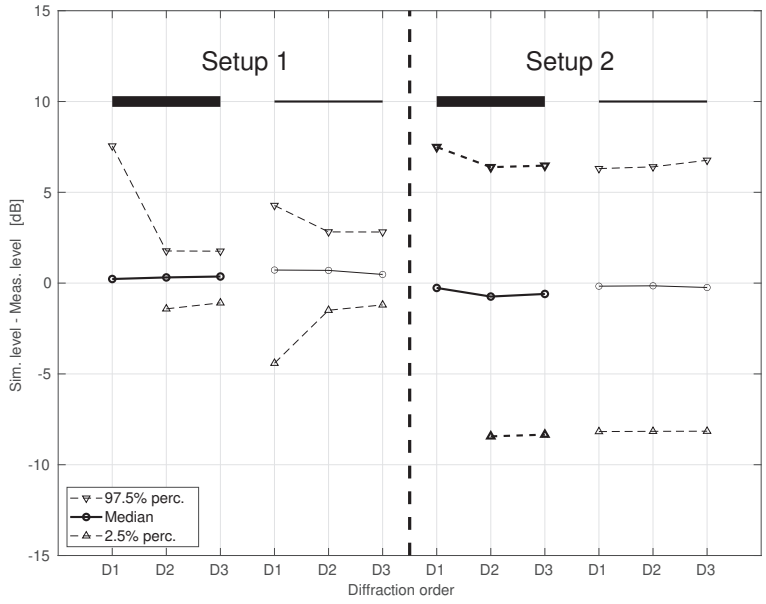

Figure 6: Median and percentiles of the difference between measured and simulated results. The values are calculated with 1/6th-octave band smoothing, and 1/6th-octave band sampling, for each simulation case: thin and thick plate, and diffraction order 1-3. The setup and plate thickness is indicated above the curves in the figure while the diffraction order is indicated on the horizontal axis.

Fig. 6 suggests that measurement setup 1 has generally been simulated with greater accuracy than setup 2. The median values are very similar, within $\pm$ 1 dB for all diffraction orders, for both setups 1 and 2. However, the spread in agreement, illustrated by percentile values, is substantially greater for setup 2 than for setup 1. We draw the intermediate conclusion that the positioning uncertainty was higher for setup 2 than for setup 1. In this short paper, we focus on setup 1. For setup 1 one can also make a few observations. First, diffraction order 1 gives less accuracy for both the thin and thick plate modeling. Second, using the thick plate model gives greater accuracy.

6.1. Frequency dependence of results

In Fig. 6, results for all frequency bands were pooled together. However, it can be assumed that the difference between simulations and measurements is larger for middle and higher frequencies than for lower, for several reasons. One reason is that a certain uncertainty of the plate dimension, and of the transducer positioning, leads to larger and larger uncertainties for interference effects as the wavelength gets shorter. Another reason is that the used loudspeaker and, to a smaller degree, microphone, show directivity effects above some frequency. The interference effects would largely be smoothed out and be smaller for octave-band smoothed responses than for fractional-octave band smoothed results. Fig. 7 show the octave-band and 1/6th octave-band smoothed results,

and the variation range, expressed as the 95%-range, increases gradually from around 4 kHz. Also, the median values in Fig. 7(b) indicate a systematic overestimation that gradually increases from around 600-1000 Hz, up to 1 dB around 10-20 kHz. This gradual increase might be caused by the slowly increasing directivity of the used loudspeaker element. For each frequency value in Fig. 7, the results for 12 different angles contribute to the median and percentile values.

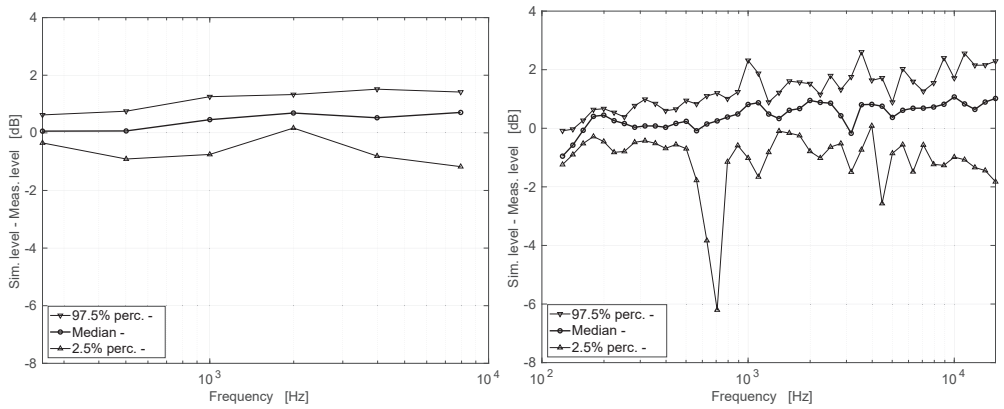

(a) (b)

Figure 7: Simulated level - measured level as function of frequency, for (a) octave-band smoothed responses, and (b) 1/6-th octave band smoothed responses. Results are shown only for setup 1, and for the simulations using a thick plate model, and third-order diffraction.

6.2. Thin vs. thick plate

The plate used in the measurements had a size of 1 m by 1 m, and a thickness of 20 mm. It seems reasonable that the plate could be modeled thin or thick for low frequencies, but that a thin plate modeling might be inadequate at high frequencies. To investigate that, Fig. 8 shows the median and percentiles of the difference between simulations and measurements, using both thick and thin plate, as a function both of frequency and angle.

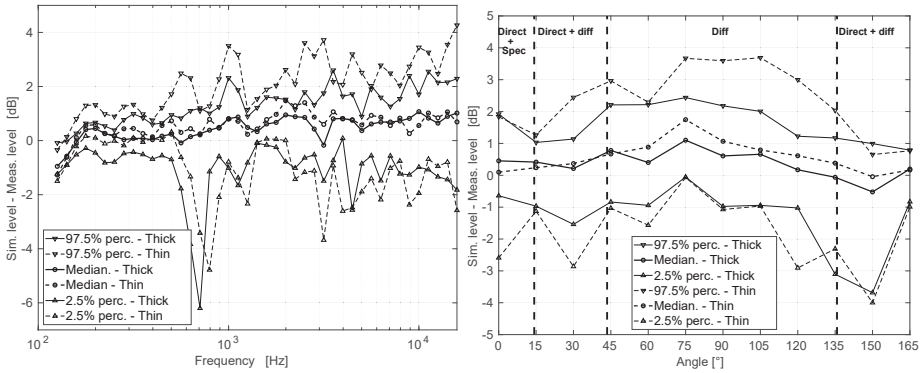

(a) (b)

Figure 8: Median and percentiles of the difference between simulated and measured levels for the thin and the thick plate model, for source-receiver position 1 and diffraction order 3, 1/6th-octave band frequency smoothing, (a) as function of frequency, and (b) as function of angle. Dashed lines indicate which angles represent different combinations of soundpaths.

In Fig. 8 a), the median values vary between 0 dB and 1 dB (up to 1.5 dB for the thin plate), and no clear difference can be observed between the thin and the thick plate results. For the most part both percentile figures

are closer to zero for the thick plate across the spectrum. There is no clear tendency that the thick plate results are more accurate than the thin plate results for the higher frequencies. When the comparison is plotted as function of plate angle, in Fig. 8 b), it can be observed that the differences, for both the thin and the thick plate, tend to be more positive for the plate angles where only diffraction occurs. A positive difference implies that the simulated levels were higher than the measured ones, which is consistent with a directional loudspeaker - the sound radiated from the measurement loudspeaker towards the edges was somewhat weaker than for a truly omnidirectional loudspeaker. For the plate angle 90 degrees, one of the four edges of the plate will be hit by a wave radiated at 30 degrees radiation angle from the loudspeaker and therefore the influence of the loudspeaker directivity would be strongest around the 90 degree plate angle.

7 Uncertainties

During the measurements, great care was taken to determine the positions of the source, receiver and plate. It was estimated that the coordinates of the source, receiver and plate centre could be determined with an accuracy of $\pm$ 2 mm. The coordinates of the corners of the plate have a higher degree of uncertainty for two reasons. First, the plate was rotated by hand, using a large protractor placed on the floor beneath the plate and vertical laser to aim the plate at the desired angle. This operation was both tedious and difficult to get right. In a separate study, where simulations of the plate were repeated with the plate rotated in steps of 0.1° around the *nominal* rotation angle in the measurements indicated that the error associated with the rotation angles might have been up to $\pm$ 1.2°, which for a plate of a 1 m size translates to $\pm$ 10 mm. Second, the plate itself was measurably skewed, by a few mm, which is difficult to simulate in the current version of the ED toolbox. It is difficult to estimate the total error of these sources of uncertainty, but it is reasonable to estimate the total positioning uncertainties to be on the order of $\pm$ 5-20 mm. The reason for the manual adjustment of the rotation of the plate was a desire for the suspension of the plate to be as thin as possible, minimizing spurious reflections. However, the difficulties associated with the adjustments suggest that the advantages with the increased precision of an electronic turntable might outweigh the disadvantages of spurious reflections.

The second greatest error source is the sound speed, as it affects the arrival of the different components in the impulse response. The greatest influence on the sound speed in this case is the temperature, which was recorded before and after each measurement. The range of the different temperatures recorded was 2 degrees, from 16,9 to 18,9 degrees Celsius. This gives rise to the sound speed varying between 342,05 m/s to 343,30 m/s. The simulations though were performed with the temperature of 18 °C for all measurements and thus the simulated sound speed was set to 342.74 m/s.

8 Conclusions

Measurements and simulations of reflections from a 1x1 m plate rotated around its vertical axis in increments of 15 degrees have been performed. Numerical edge-diffraction based simulations were performed with both a thin and a thick plate model.

The most important, and unsurprising, finding is that the inclusion of second and higher order diffraction improved the accuracy of the simulations substantially, especially for the case of the thick plate. When looking at the difference between measured and simulated levels, see Fig. 8, the thick plate for the most part performs better than the thin plate across the spectrum. Naturally the thick plate is performing worse than the thin plate for first order diffraction, as the cases where the direct path between source and receiver is obstructed produce no sound in the simulations. The most accurate simulation results were found for the thick plate model, diffraction order 3, and source-receiver setup 1. Across 516 comparisons of 1/6th-octave band levels, from the 125 Hz band to the 16 kHz band, and 12 plate angles, the 2.5% and 97.5% percentiles were -1.1 dB and +1.8 dB, respectively, with a median value of 0.36 dB. For diffraction order 2, these results were only marginally worse,

with the percentile values -1.4 dB and +1.8 dB. Uncertainties associated with the exact positioning of the plate have affected the results to a non-negligible degree. Also, the loudspeaker element's directivity have probably also affected the results to some degree. Further measurements of this type will be performed with the inclusion of a electronic turntable to reduce the amount of plate position error, at the cost of more spurious reflections.

Acknowledgements

The authors would like to thank Tim Cato Netland for assistance in the preparations for, and conduction of, the measurements.

References

[1] Lauri Savioja and U. Peter Svensson. Overview of geometrical room acoustic modeling techniques. *The Journal of the Acoustical Society of America*, 138(2):708–730, 2015. doi: 10.1121/1.4926438. URL https://doi.org/10.1121/1.4926438.

[2] U. P. Svensson, R. I. Fred, and J. Vanderkooy. An analytic secondary source model of edge diffraction impulse responses. *The Journal of the Acoustical Society of America*, 106(5):2331–2344, 1999. doi: http://dx.doi.org/10.1121/1.428071. URL http://scitation.aip.org/content/asa/journal/jasa/106/5/10.1121/1.428071.

[3] Fabian Brinkmann, Lukas Aspöck, David Ackermann, Steffen Lepa, Michael Vorländer, and Stefan Weinzierl. A round robin on room acoustical simulation and auralization. *The Journal of the Acoustical Society of America*, 145(4):2746–2760, 2019. doi: 10.1121/1.5096178. URL https://doi.org/10.1121/1.5096178.

[4] Trevor J Cox and YW Lam. Evaluation of methods for predicting the scattering from simple rigid panels. *Applied Acoustics*, 40(2):123–140, 1993.

[5] J. J. Rindel. Attenuation of sound reflections due to diffraction. In *Proceedings of the Nordic Acoustical Meeting, Aalborg, Denmark*, 1986.

[6] U. Peter Svensson. Edge diffraction toolbox for matlab, v. 0.216 [computer program]. . URL https://github.com/upsvensson/Edge-diffraction-Matlab-toolbox.

[7] A. Asheim and U. P. Svensson. An integral equation formulation for the diffraction from convex plates and polyhedra. *The Journal of the Acoustical Society of America*, 133(6):3681–3691, 2013. doi: http://dx.doi.org/10.1121/1.4802654.

[8] Svensson U. P. Torres, R. R. and M. Kleiner. Computation of edge diffraction for more accurate room acoustics auralization. *The Journal of the Acoustical Society of America*, 109(1):600–610, 2001. doi: http://dx.doi.org/10.1121/1.1340647.

[9] U. Peter Svensson, Paul T. Calamia, and Shinsuke Nakanishi. Frequency-domain edge diffraction for finite and infinite edges. *Acta Acustica united with Acustica*, 95:568–572, 2009.

[10] U. Peter Svensson. Edge diffraction toolbox for matlab, version edb1 [computer program]. . URL https://folk.ntnu.no/ulfps/software/index.html.

[11] A. Lovstad and U. P. Svensson. Diffracted sound field from an orchestra pit. *Acoust. Sci. Tech.*, 26:237–239, 2005.